Report

Current Biology

Natural binocular depth discrimination behavior In mice explained by visual cortical activity

Highlights

- Mice require binocular vision to perform a novel task of depth discrimination
- Task performance provides a psychophysical range of mouse depth discrimination
- Discrimination based on disparity using binocular neurons in V1 matches behavior
- Neuronal discrimination from disparity is robust to changes in binocular alignment

Authors

Howard C. Boone, Jason M. Samonds, Emily C. Crouse, Carrie Barr, Nicholas J. Priebe, Aaron W. McGee

Correspondence

nico@austin.utexas.edu (N.J.P.), aaron.mcgee@louisville.edu (A.W.M.)

In brief

Boone et al. estimate the psychophysical range of depth discrimination for mice with a modified cliff task. They demonstrate mice require binocular vision to perform the task and identify that disparity information from populations of neurons in visual cortex is sufficient to predict performance across a range of depths.

Boone et al., 2021, Current Biology *31*, 1–8
May 24, 2021
https://doi.org/10.1016/j.cub.2021.02.031

CellPress

Please cite this article in press as: Boone et al., Natural binocular depth discrimination behavior In mice explained by visual cortical activity, Current Biology (2021), https://doi.org/10.1016/j.cub.2021.02.031

Current Biology

CellPress

Report

Natural binocular depth discrimination behavior In mice explained by visual cortical activity

Howard C. Boone,[1,3] Jason M. Samonds,[2,3] Emily C. Crouse,[1] Carrie Barr,[2] Nicholas J. Priebe,[2,*] and Aaron W. McGee[1,4,*]
[1]University of Louisville, School of Medicine, Department of Anatomical Sciences and Neurobiology, 511 S. Floyd St., Louisville, KY 40202, USA
[2]The University of Texas at Austin, Center for Learning and Memory and The Institute for Neuroscience, 100 E 24th St., Austin, Texas 78712, USA
[3]These authors contributed equally
[4]Lead Contact
*Correspondence: nico@austin.utexas.edu (N.J.P.), aaron.mcgee@louisville.edu (A.W.M.)
https://doi.org/10.1016/j.cub.2021.02.031

SUMMARY

In mice and other mammals, forebrain neurons integrate right and left eye information to generate a three-dimensional representation of the visual environment. Neurons in the visual cortex of mice are sensitive to binocular disparity,[1–3] yet it is unclear whether that sensitivity is linked to the perception of depth.[4–8] We developed a natural task based on the classic visual cliff and pole descent tasks to estimate the psychophysical range of mouse depth discrimination.[5,9] Mice with binocular vision descended to a near (shallow) surface more often when surrounding far (deep) surfaces were progressively more distant. Occlusion of one eye severely impaired their ability to target the near surface. We quantified the distance at which animals make their decisions to estimate the binocular image displacement of the checkerboard pattern on the near and far surfaces. Then, we assayed the disparity sensitivity of large populations of binocular neurons in primary visual cortex (V1) using two-photon microscopy[2] and quantitatively compared this information available in V1 to their behavioral sensitivity. Disparity information in V1 matches the behavioral performance over the range of depths examined and was resistant to changes in binocular alignment. These findings reveal that mice naturally use stereoscopic cues to guide their behavior and indicate a neural basis for this depth discrimination task.

RESULTS AND DISCUSSION

Disparity selectivity is associated with binocular depth perception.[10] Although mice can discriminate binocular disparities after training over weeks[2], it is unknown whether mice naturally use this binocular information and whether their natural behavioral sensitivity to depth matches their neural sensitivity to disparity. Previous behavioral work has demonstrated that mice are able to judge the distance of objects, but it is unclear whether monocular depth cues, such as size and motion parallax, or binocular cues, such as disparity, are employed in these tasks.[5] To assay whether mice use binocular information to infer depth without training, we modified the classical visual cliff test,[5] in which an animal is placed on glass over surfaces with shallow and deep locations, to include a pole descent to the surfaces.[9] The classical visual cliff test relies on visual activity from the lower visual field, where there is less binocular overlap (Figure 1A). We incorporated the pole descent because it orients mouse eyes toward the surfaces to discriminate and engages the upper visual field, where there is considerable binocular overlap in visual representations (Figure 1A and Figure S1; related to Figure 1).[2,11,12]

In the pole descent cliff task (PDCT), a mouse descends a vertical pole to the glass divided into four quadrants. One quadrant is closer, with a 2.5 cm surface below the cone, whereas the other quadrants had surfaces with adjustable deeper depths. A cone 10 cm in diameter rests at the bottom of the pole on thin metal rails 2 cm above a plate of glass and 2.5 cm above the nearest platform (Figure 1B and Figure S2 related to Figure 1). These rails obscure the edges between the quadrant presenting the nearest platform and the remaining three quadrants. All interior surfaces are covered by a black and white 2.5 cm checkboard pattern.

We tested cohorts of mice on the PDCT with the nearest platform fixed at 2.5 cm below the cone and one of four distances for the remaining three quadrants: 7.6 cm, 15.2 cm, 30.5, or 61 cm (Figure 1C). The fractional success of individual mice exiting the cone to the quadrant of the nearest platform rather than the other three quadrants was determined from 10–15 interleaved trials (see STAR Methods for details). Mice with binocular vision did not preferentially target the nearest platform when the remaining three quadrants were 7.6 cm below the cone ($p > 0.99$, Kruskal-Wallis test with Dunn's correction for 7 comparisons included comparing each distance pair between binocular and monocular vision as well as the fractional success of monocular vision of 2.5 versus 7.6 cm versus the remaining 3 distance pairs) (Figure 1C). Mice displayed greater preference for the nearest platform when the other platforms were located at distances of 15.2 cm or greater ($p = 0.0002$ or less for each comparison,). Mice tested

Please cite this article in press as: Boone et al., Natural binocular depth discrimination behavior In mice explained by visual cortical activity, Current Biology (2021), https://doi.org/10.1016/j.cub.2021.02.031

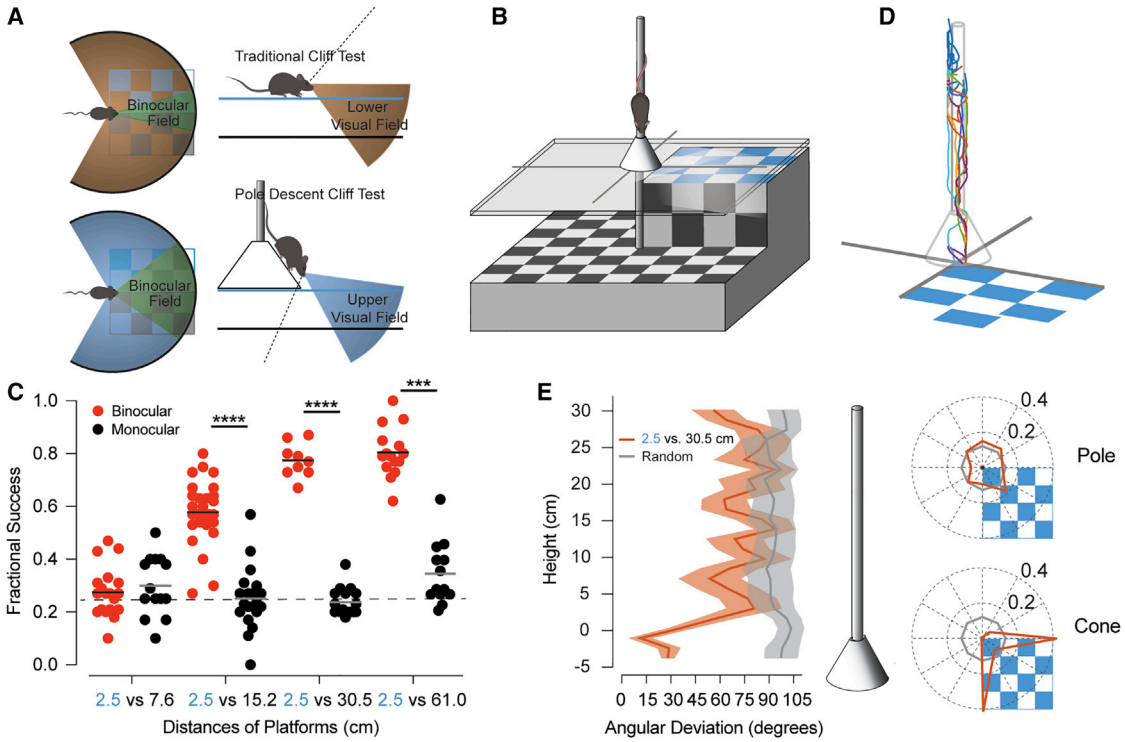

Figure 1. The pole descent cliff task reveals the binocular component of depth perception

(A) The orientation of mouse eyes results in greater binocular overlap (green) in the upper (blue) versus the lower (brown) visual field. Traditional cliff tests orient the mouse parallel to the discriminated surfaces, which will be mostly represented in the lower visual field. The pole descent reorients the mouse downward so that the discriminated surfaces are mostly in the upper visual field.

(B) A schematic of the pole descent cliff task. Mice descend a pole 1 cm in diameter to cone positioned above a plate of glass. Small aluminum rails obscure the edges beneath separating the quadrant with the nearest platform from the three more distant surfaces. The entire interior surface of the box is covered in a black and white checkerboard pattern, including the walls (not shown).

(C) Fractional success of mice under either binocular (red) or monocular viewing conditions (black) descending to the nearest platform fixed at 2.5 cm relative to the distance of the remaining platforms at 7.6 cm (n = 19 binocular, 14 monocular), 15.2 cm (n = 28,20), 30.5 cm, = (n = 9,17) and 61.0 cm (n = 15,13). Each mouse (circle) was tested 10–15 times at only one pair of depths and either binocular or monocular vision. Dashed line is a chance fraction of 0.25. (***p = 0.0002; ****p < 0.0001, Kruskal Wallis test).

(D) A sample of three-dimensional traces of the position of the mouse descending the pole over time when exiting to the 2.5 versus the 30.5 cm surface. Each color is a different trial.

(E) Left: angular position around the pole with respect to the near surface varies substantially until the mice reach the cone after descending the pole. Middle: shaded regions are standard error. Right: the angular position is similar to a random distribution on the pole (upper) and is biased toward the edges within the quadrant of the near surface when the mice reach the cone (lower). See also Figures S1, S2, and Videos S1 and S2.

with monocular vision by suturing closed one eye exhibited no significant choice preference for platform distance ($p > 0.99$, comparing fractional success of monocular 2.5 versus 7.6 against each greater distance). We measured the time required for a subset of mice to descend the pole with either binocular or monocular vision. The percentage of discarded trials (slips or time-outs) for monocular versus binocular trials were similar, and the mice did not descend the poles at significantly longer times when one eye was occluded (Mann-Whitney test, $p = 0.23$, data not shown), suggesting that the occlusion did not affect their ability to descend the pole. Thus, mice require binocular vision to identify the nearest platform in the PDCT.

For a subset of trials, we recorded video of the mice descending the pole and estimated their position in three dimensions (Figure 1D and Videos S1 and S2; related to Figure 1). When the mice chose the near quadrant, the mice appeared to make their decision when they reached the cone (Figure 1E). We quantified this observation by measuring the angular deviation of the position around the pole versus the distance from the cone, which drops significantly when reaching the cone (Figure 1E). The position of the mice on the pole with respect to the near surface appears random but narrows near the borders for the quadrant of the near surface when the mice reach the cone (Figure 1E). This reorientation when mice are close to the surfaces, where binocular disparity differences would be larger, supports that they make their decision close to this location.

Next, we examined how these behavioral results relate to the tuning of visual cortical neurons to horizontal binocular disparities associated with depth. Objects nearer with respect to aligned binocular receptive fields have crossed disparities (negative) while more distant objects have uncrossed disparities (positive) (Figures 2A and 2B). We converted the distances of the surfaces presented in the PDCT into disparities based on the geometry for the interocular separation of the mouse (1 cm). The

Please cite this article in press as: Boone et al., Natural binocular depth discrimination behavior In mice explained by visual cortical activity, Current Biology (2021), https://doi.org/10.1016/j.cub.2021.02.031

CellPress

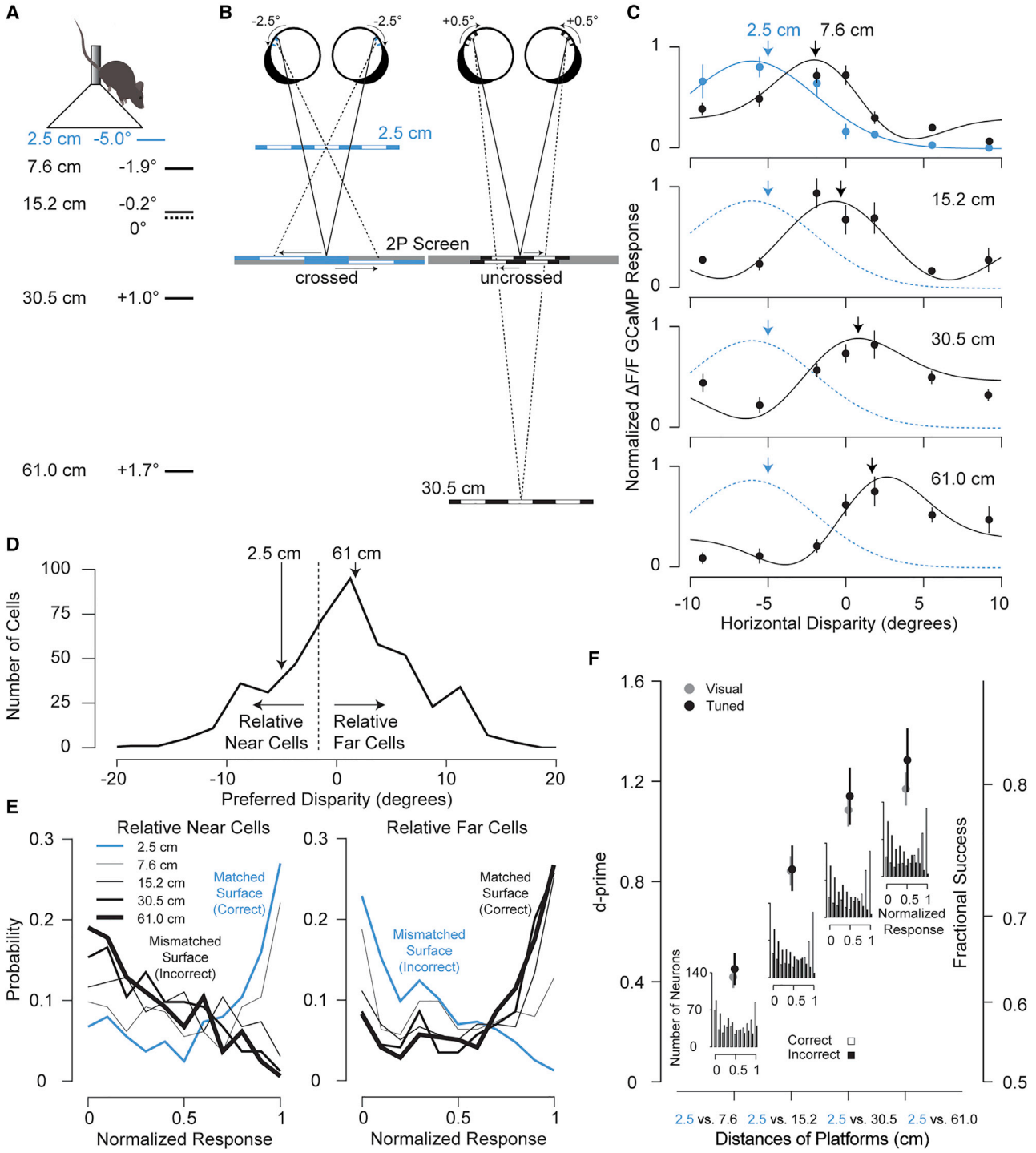

Figure 2. Neuronal discrimination of PDCT depths with disparity-tuned neurons in the mouse visual cortex

(A) Binocular disparity for the mouse was computed for each surface depth used in the pole descent cliff task (PDCT). The dashed line corresponds to zero disparity for the viewing distance.

(B) An example of retinal projections for 2.5 and 30.5 cm surfaces is shown to the right. The gray screen shows the horizontal shift for the left (upper) and right (lower) eye images necessary to produce stereoscopic surfaces that correspond to the depths of these PDCT surfaces. The projections are not drawn to scale for clarity.

(C) Example disparity tuning curves measured with two-photon microscopy with preferred disparities matching the PDCT surfaces. Error bars are standard error (n = 10 repeats).

(legend continued on next page)

Please cite this article in press as: Boone et al., Natural binocular depth discrimination behavior In mice explained by visual cortical activity, Current Biology (2021), https://doi.org/10.1016/j.cub.2021.02.031

nearest surface yields a crossed disparity of 5 degrees while the farthest surfaces start to asymptote at uncrossed disparities of nearly 2 degrees (Figure 2A). This range of disparities is well within the tuning preferences of mice.[2,3]

In this framework, we evaluated whether the calcium responses for a population of neurons from the visual cortex imaged by two-photon microscopy were sufficient to discriminate surfaces for the distances presented for the PDCT (Figure 1C). Figure 2C presents example disparity tuning curves of neurons across the distances tested with the PDCT. Tuning curves for 2.5 and 7.6 cm have a substantial amount of overlap and only modest differences in responses. The differences in responses increases as the distance between surfaces increases until the disparity differences begin to saturate near the limit for a convergence angle for the greatest distances.

The distances tested in the PDCT cluster around the disparities to which most neurons are tuned (Figure 2D). To test discrimination with these neuronal responses, we divided the population of neurons into those that prefer relative near surfaces from neurons preferring relative far surfaces. Relative near and far are defined by splitting the population based on the PDCT distances. Similar to Britten et al.,[13] the population of neurons are performing a two-alternative forced choice task. Relative-near neurons prefer the near surface (2.5 cm) and all other surfaces are mismatched to this preference or are ''anti-preferred'' surfaces (Figure 2E, left). Relative-far neurons prefer the far surfaces, and the near surface is mismatched or anti-preferred (Figure 2E, right). If the relative-near neurons are highly responsive and relative-far neurons are not responsive, the near surface is discriminated. If relative-far neurons are highly responsive and relative near-neurons are not responsive, the far surface is discriminated. For all neurons in the population, we computed d' between pairs of responses for surfaces matched to the preferred surface (correct) and responses for surfaces mismatched to the preferred surface (incorrect).[14] Estimates of d' increase systematically with increasing differences in distance and plateau for the most distant surfaces (Figure 2F). This outcome was similar whether we evaluated only neurons that are significantly tuned for disparity (tuned) or all neurons that displayed significant visually evoked responses (visual). The results are similar between significant disparity-tuned neurons and visually responsive neurons because many visually responsive neurons are still selective for disparity but do not pass a significance test for disparity because of the variable response of simple cells to random dot stimuli.[2,15] The d' values for neuronal discrimination correspond to values of fractional success that are similar to the fractional success we measured with the PDCT (Figure 2F). These findings are consistent with a role for disparity tuning in binocular performance on the PDCT.

We determined the disparities for each depth for mice viewing the surface 5.1 cm from the edge of the cone (Figure 3A, brown mouse). We selected this viewing distance based on observations of the behavior of the mice because it is where they frequently changed their direction toward the quadrant of the near surface (Figure 1E). However, these d' values are resistant to reasonable deviations in the viewing position. We repeated our discrimination analysis using distances progressively nearer to and farther away from the edge of the cone as the base of the pole. Mice viewing the surfaces from higher on the cone reduces the convergence angle and constricts disparities over a narrower range, leading to greater overlap in disparity tuning curves (Figure 3A, light blue and blue). This results in lower d' values and reduced discrimination performance but with a similar trajectory (Figure 3B). This potentially explains why the mice would wait until the cone to choose a quadrant, since disparity discrimination performance would continue to improve as they move closer. Mice viewing the surfaces from closer to the edge of the cone increases the convergence angle and expands the disparity differences (Figure 3A, pink and red). This results in slightly higher d' values and enhanced discrimination performance (Figure 3B). At the closest viewing distance tested (Figure 3A, dark red), performance is reduced because the disparity of the nearest surface extends to the edge of the distribution of preferred disparities (<-10 degrees) where fewer neurons are activated (Figure 3B).

Our discrimination analysis with respect to viewing distance in Figure 3 predicted that performance would be cut nearly in half with respect to a chance ratio of 0.5 for the optimally close distance versus the farthest distance we examined. We conducted an additional experiment to test this prediction by moving the 2.5 cm surface to 10.2 cm and the 30.5 cm surface to 38.1 cm. This forced the mice to make a depth discrimination from farther away. The mice were still able to significantly discriminate a 10.2 versus 38.1 cm surface above chance (0.45 ± 0.04; Kruskal Wallis test, $p = 0.002$, $n = 17$ mice), but that performance was significantly lower (less than half with respect to a chance ratio of 0.25) than mice discriminating a 2.5 versus 30.5 cm surface (0.77 ± 0.02; Kruskal Wallis test, $p = 0.03$) (Figure S3, related to Figure 3).

Binocular eye movements differ between head-fixed mice and freely behaving mice.[16] When mice make saccadic eye or head/eye movements, any asymmetry in saccade sizes changes binocular alignment (Figure 4A). The spread of this distribution doubles for mice that are freely moving (black; $\sigma = 7.9°$)[16] compared to head-fixed mice (gray; $\sigma = 3.9°$).[2,16] To examine how the greater range of natural eye movements may influence depth perception, we repeated our disparity discrimination with different binocular alignments. We used the 10th, 25th, 75th, and 90th percentile alignments to compute new disparities for the PDCT surfaces (Figures 4A and 4B). When the eyes rotate inward (less divergent), the surfaces are represented by more uncrossed disparities. When the eyes rotate outward (more divergent), the surfaces are represented by more crossed disparities. Disparities associated with each of the four eye alignments are captured by the

(D) Distribution of disparity tuning preferences for neurons in the visual cortex. The unimodal distribution was divided (dashed line) into relative near and far tuned based on the PDCT disparities.[2,9]

(E) Distribution of normalized responses for relative near- and far-tuned neurons for each surface.

(F) Neuronal discrimination measured with d' between normalized responses to the two compared surfaces for significant disparity-tuned neurons (Tuned, N = 172) and significant visually responsive neurons (Visual, N = 477). Fractional success was estimated from d'. Insets are combined distributions of correct and incorrect responses for relative near- and far-tuned cells. Error bars are standard error and all data points are statistically significantly greater than zero (bootstrapped, $p < 0.001$).

Please cite this article in press as: Boone et al., Natural binocular depth discrimination behavior In mice explained by visual cortical activity, Current Biology (2021), https://doi.org/10.1016/j.cub.2021.02.031

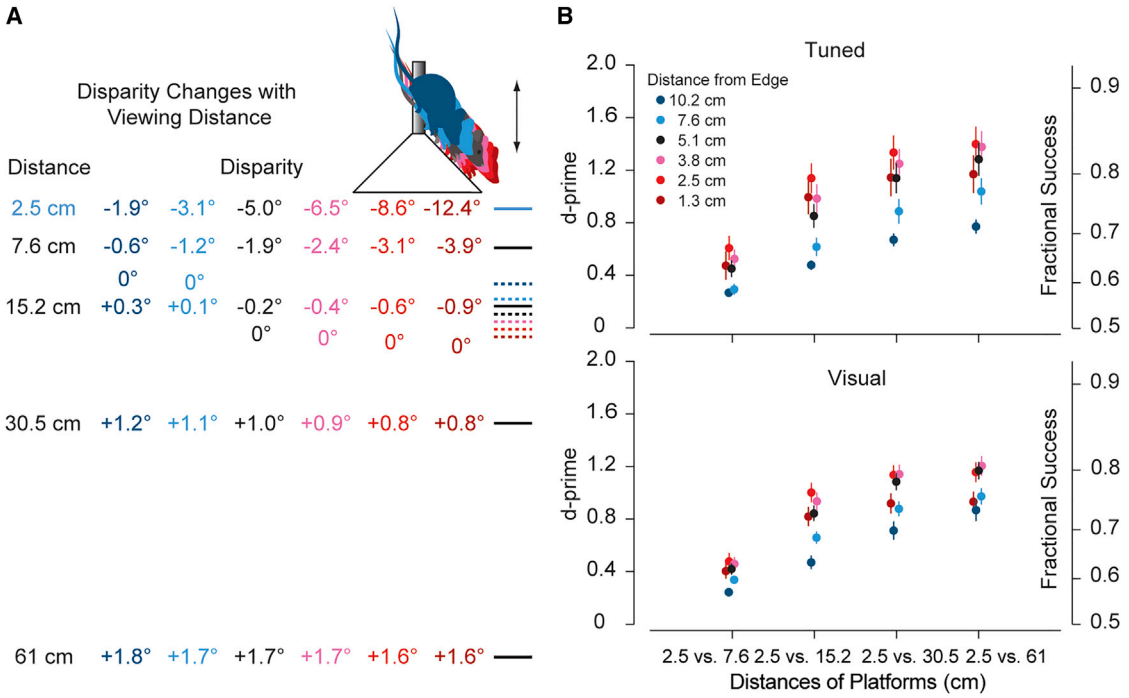

Figure 3. Robustness of neuronal discrimination with changes in viewing distance

(A) Surface depths were converted into binocular disparity for a range of viewing distances from farther to nearer (blue to red). Dashed lines are zero disparity for each corresponding viewing distance defined by the screen distance used when measuring disparity tuning (22.2 cm).

(B) Neuronal discrimination performance for different viewing distances for significant disparity-tuned (top) and visually responsive (bottom) neurons. Error bars are standard error. See also Figure S3.

distribution of preferred disparities we have reported previously (Figure 4B).[2] The discrimination performance is nearly identical for the 25th and 75th percentile, suggesting that there would be no change in performance for half of the observed natural binocular alignments (Figure 4C, pink and light blue). Performance begins to diminish for the most convergent and divergent alignments, but the discrimination still follows a similar trajectory (Figure 4C, red and blue). Performance is diminished for these alignments because they move disparities for the nearest and farthest surfaces to the edges of the distribution where fewer neurons will be activated by these surfaces. If we apply a minimum threshold that considers only those neurons sufficiently activated by the surfaces during the task, neuronal discrimination performance can be enhanced to better match the behavioral performance (Figure S4, related to Figure 4).

Mice are natural climbers[17,18]. Here, we exploited that natural climbing behavior to investigate the characteristics of depth perception in mice. We modified the classic visual cliff task by introducing a pole descent component in order to measure the ranges of depths that mice can discriminate behaviorally without training. Using this paradigm, we demonstrate that mice perform above chance levels at finding the nearest surface when comparing distances between 2.5 cm and 15.1 cm, and performance progressively improves with larger differences in distances. This performance was severely impaired by monocular occlusion, consistent with mice using binocular vision to perform the task.

A key advantage of the PDCT is that it orients the mouse toward the surfaces of the platform (Figure 1A). A consequence of the lateral and upward orientation of mouse eyes is that most of their binocular overlap occurs in the upper visual field.[2,11,12] Traditional cliff tests place mice on a horizontal transparent surface or rod just above the surfaces.[5,19,20] These tasks generally orient the mouse parallel to the plane of the surfaces at differing depths. Rodents tilt their head downward about 20 degrees to position the binocular field in front of them.[7,21] This angle is much smaller than the 90-degree change in orientation associated with descending the pole. When the mice are oriented horizontally, surfaces are predominantly confined to the lower visual field, where there is much less binocular overlap compared to our task. In the classical test of depth perception, mice have less access to binocular information and may therefore depend more on monocular depth cues such as shadows, motion parallax, or perspective from differences in size. We demonstrate that PDCT requires binocular vision and that their performance matches expectations from the neural disparity signals. The placement of animals on a pole provides a paradigm in which they naturally take advantage of disparity cues.

Binocular overlap is one of several features that vary across the dorsal-ventral axis of visual space for the mouse.[22] The ventral retina is dominated by cones sensitive to ultraviolet light.[23,24] Retinal ganglion cells (RGCs) also vary in function, cell density, and morphology across this axis. For example, transient off-alpha RGCs are more sustained in the dorsal retina compared to the ventral retina,[25] and direction-selective JAM-B RGCs become color opponent in the ventral retina.[26] The density of W3 RGCs is

Please cite this article in press as: Boone et al., Natural binocular depth discrimination behavior In mice explained by visual cortical activity, Current Biology (2021), https://doi.org/10.1016/j.cub.2021.02.031

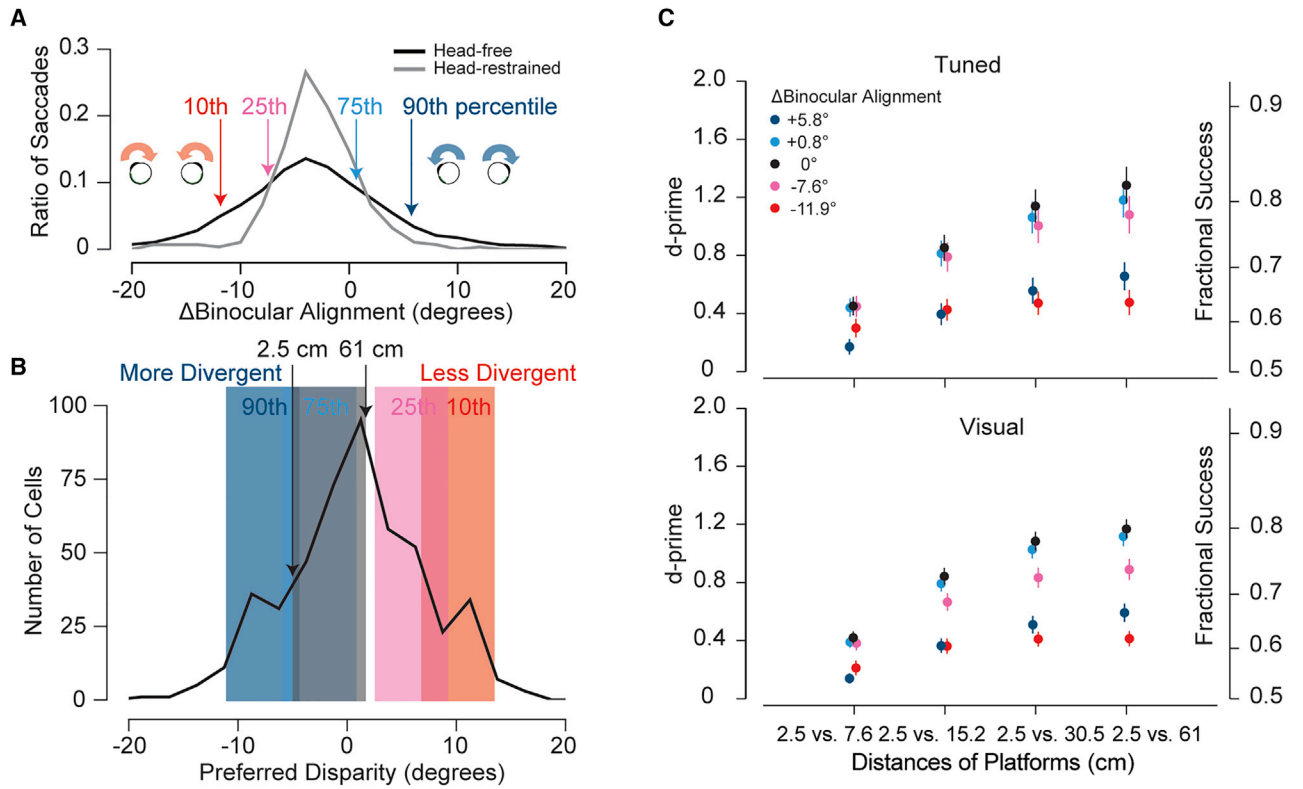

Figure 4. Robustness of neuronal discrimination with changes in binocular alignment

(A) Distribution of saccade size differences for head-fixed and head-free freely moving mice.[16] A negative difference corresponds to the eyes rotating inward (left, red) and a positive difference corresponds to the eyes rotating outward (right, blue). Arrows highlight percentiles of the data that were used to test performance for changes in binocular alignment.

(B) Distribution of preferred disparities for all significant visually response neurons.[2] Highlighted regions correspond to the disparity range represented by the surfaces used in the task for the average binocular alignment (gray) and corresponding changes in alignment noted in (C).

(C) Neuronal discrimination performance for different binocular alignments for significant disparity-tuned (top) and visually responsive (bottom) neurons. Error bars are standard error. See also Figure S4.

greater in the medioventral retina, and these RGCs are selective for small moving objects.[27] Both orientation-selective JAM-B RGCs and posterior tuned on-off direction selective ganglion cells display shifts in morphology in the ventral retina.[28,29] How this diversity of retinal function translates into variation in spatio-temporal coding of the visual scene to contribute to visually guided performance such as the depth perception examined here are interesting but unanswered questions.

In previous work, we demonstrated that mice could use binocular disparity cues in trained behavior.[2] However, this task was unnatural and required head-fixed mice and extensive training for a rewarded behavior. Here, we tested depths in the PDCT that correspond to most of the preferred disparities of binocular neurons in mouse visual cortex. Critically, disparity responses associated with surfaces matching the distances examined in the PDCT were sufficient to discriminate depth with performance that matched the behavior. The range of disparity tuning and limits (threshold and saturation) in discrimination in the visual cortex correspond to the range and limits of depths discriminated by the mice. Additionally, our neural discrimination analysis predicted diminished performance from greater viewing distances, a prediction borne out in subsequent behavioral experiments (Figure S3, related to Figure 3).

Binocular eye movements differ between head-fixed mice and mice engaged in natural behaviors.[16] Whether the stereoscopic behavior we observed with head-fixed mice would translate to natural behavior observed in rodents in general was unclear.[6–8] Although variation in binocular alignment alters the disparities of the surfaces across distance, the range of disparity preferences represented in mouse visual cortex is sufficient for nearly all possible depths encountered by mice (from 2 cm to ¥), even with large changes in binocular alignment.[2,3] Our analysis assumes that mice are making a relative disparity discrimination choosing the nearest surface in a comparison. The observation that mice generally move toward the borders between the near and far surfaces supports this assumption (Figure 1E). Because we only measured absolute disparity in V1 and our analysis makes a relative disparity discrimination, future studies will be required to examine if relative disparity is also explicitly represented in V1, or in subsequent visual areas in the mouse that have disparity tuning such as area LM.[3] In the primate visual system, relative disparity compared to absolute disparity is more strongly represented in V2 versus V1.[30,31] Disparity tuning differences between V1 and LM observed thus far in the mouse are similar to those observed between V1 and V2 in the primate.[32]

This emergence of depth perception from binocular vision has been the subject of intense scrutiny as a platform to understand how neural circuits perform computations and are subject to sensory experience. We developed a novel assay of depth sensitivity, demonstrated that mice require binocular cues to solve this task, and linked the performance in this task to the neural signals of disparity in the visual cortex. Because performance on this task is closely aligned with the cortical visual representation, it may prove to be a useful tool to understand the behavioral consequences that follow abnormalities in binocular vision including amblyopia, as well as an assay to measure the effectiveness of treatments to assist in the recovery of normal binocular vision.

STAR★METHODS

Detailed methods are provided in the online version of this paper and include the following:

- KEY RESOURCES TABLE
- RESOURCE AVAILABILITY
  - Lead Contact
  - Materials Availability
  - Data and Code Availability
- EXPERIMENTAL MODEL AND SUBJECT DETAILS
  - Mice
- METHOD DETAILS
  - Monocular Deprivation (MD)
  - Whisker clipping
  - The Pole Descent Visual Cliff Task
  - Videography of the Pole Descent Cliff Task
  - Calcium imaging of neuronal activity with two-photon microscopy
  - Neuronal discrimination of depth
- QUANTIFICATION AND STATISTICAL ANALYSIS

SUPPLEMENTAL INFORMATION

Supplemental Information can be found online at https://doi.org/10.1016/j.cub.2021.02.031.

ACKNOWLEDGMENTS

This research is supported by the National Eye Institute to N.J.P. (EY025102) and A.W.M. (EY021580)

AUTHOR CONTRIBUTIONS

The contributions are as follows: H.C.B. and E.C.C. performed behavioral assays. H.C.B. recorded videos of task performance. J.M.S., C.B., and N.J.P. quantified task performance in videos. J.M.S. converted PDCT distances into disparities and performed the neuronal discrimination analyses. J.M.S., H.C.B., N.J.P., and A.W.M. wrote and revised the manuscript.

DECLARATION OF INTERESTS

The authors declare no competing interests.

Received: November 23, 2020
Revised: January 20, 2021
Accepted: February 15, 2021
Published: March 10, 2021

REFERENCES

1. Scholl, B., Burge, J., and Priebe, N.J. (2013). Binocular integration and disparity selectivity in mouse primary visual cortex. J. Neurophysiol. *109*, 3013–3024. https://doi.org/10.1152/jn.01021.2012.
2. Samonds, J.M., Choi, V., and Priebe, N.J. (2019). Mice Discriminate Stereoscopic Surfaces Without Fixating in Depth. J. Neurosci. *39*, 8024–8037. https://doi.org/10.1523/Jneurosci.0895-19.2019.
3. La Chioma, A., Bonhoeffer, T., and Hubener, M. (2019). Area-Specific Mapping of Binocular Disparity across Mouse Visual Cortex. Curr. Biol. *29*, 2954-+. https://doi.org/10.1016/j.cub.2019.07.037.
4. Russell, J.T. (1932). Depth discrimination in the rat. Pedagog. Semin. J. Genet. Psychol. *40*, 136–161.
5. Fox, M.W. (1965). Visual Cliff Test for Study of Visual Depth Perception in Mouse. Anim Behav *13*, 232. https://doi.org/10.1016/0003-3472(65)90040-0.
6. Ellard, C.G., Goodale, M.A., and Timney, B. (1984). Distance estimation in the Mongolian gerbil: the role of dynamic depth cues. Behav. Brain Res. *14*, 29–39. https://doi.org/10.1016/0166-4328(84)90017-2.
7. Wallace, D.J., Greenberg, D.S., Sawinski, J., Rulla, S., Notaro, G., and Kerr, J.N. (2013). Rats maintain an overhead binocular field at the expense of constant fusion. Nature *498*, 65–69. https://doi.org/10.1038/nature12153.
8. Kautzky, M., and Busse, L. (2020). Vision: How Mice Control Their View. Curr. Biol. *30*, R635–R637. https://doi.org/10.1016/j.cub.2020.04.063.
9. Matsuura, K., Kabuto, H., Makino, H., and Ogawa, N. (1997). Pole test is a useful method for evaluating the mouse movement disorder caused by striatal dopamine depletion. J. Neurosci. Methods *73*, 45–48. https://doi.org/10.1016/s0165-0270(96)02211-x.
10. Julesz, B. (1964). Binocular Depth Perception without Familiarity Cues. Science *145*, 356–362. https://doi.org/10.1126/science.145.3630.356.
11. Dräger, U.C. (1978). Observations on monocular deprivation in mice. J. Neurophysiol. *41*, 28–42.
12. Dräger, U.C., and Olsen, J.F. (1980). Origins of crossed and uncrossed retinal projections in pigmented and albino mice. J. Comp. Neurol. *191*, 383–412. https://doi.org/10.1002/cne.901910306.
13. Britten, K.H., Shadlen, M.N., Newsome, W.T., and Movshon, J.A. (1992). The analysis of visual motion: a comparison of neuronal and psychophysical performance. J. Neurosci. *12*, 4745–4765.
14. MacMillan, N.A.C. (2005). C. D. *Detection Theory* (Lawrence Erlbaum Associates).
15. Prince, S.J.D., Pointon, A.D., Cumming, B.G., and Parker, A.J. (2002). Quantitative analysis of the responses of V1 neurons to horizontal disparity in dynamic random-dot stereograms. J. Neurophysiol. *87*, 191–208. https://doi.org/10.1152/jn.00465.2000.
16. Meyer, A.F., O'Keefe, J., and Poort, J. (2020). Two Distinct Types of Eye-Head Coupling in Freely Moving Mice. Curr. Biol. *30*, 2116–2130.e2116. https://doi.org/10.1016/j.cub.2020.04.042.
17. Dewsbury, D.A.L. (1980). D. L.; Miglietta, A. A Laboratory Study of Climbing Behavior in 11 Species of Muroid Rodents. Am. Midl. Nat. *103*, 66–72.
18. Thompson, D.B. (1990). Different Spatial Scales of Adaptation in the Climbing Behavior of Peromyscus Maniculatus: Geographic Variation, Natural Selection, and Gene Flow. Evolution *44*, 952–965. https://doi.org/10.1111/j.1558-5646.1990.tb03817.x.
19. Mazziotti, R., Baroncelli, L., Ceglia, N., Chelini, G., Sala, G.D., Magnan, C., Napoli, D., Putignano, E., Silingardi, D., Tola, J., et al. (2017). Mir-132/212 is required for maturation of binocular matching of orientation preference and depth perception. Nat. Commun. *8*, 15488. https://doi.org/10.1038/ncomms15488.
20. Gu, L., Bok, D., Yu, F., Caprioli, J., and Piri, N. (2018). Downregulation of splicing regulator RBFOX1 compromises visual depth perception. PLoS ONE *13*, e0200417. https://doi.org/10.1371/journal.pone.0200417.

21. Meister, M., and Cox, D. (2013). Rats maintain a binocular field centered on the horizon. F1000Res. *2*, 176. https://doi.org/10.12688/f1000research.2-176.v1.

22. Baden, T., Euler, T., and Berens, P. (2020). Understanding the retinal basis of vision across species. Nat. Rev. Neurosci. *21*, 5–20. https://doi.org/10.1038/s41583-019-0242-1.

23. Haverkamp, S., Wässle, H., Duebel, J., Kuner, T., Augustine, G.J., Feng, G., and Euler, T. (2005). The primordial, blue-cone color system of the mouse retina. J. Neurosci. *25*, 5438–5445. https://doi.org/10.1523/JNEUROSCI.1117-05.2005.

24. Wang, Y.V., Weick, M., and Demb, J.B. (2011). Spectral and temporal sensitivity of cone-mediated responses in mouse retinal ganglion cells. J. Neurosci. *31*, 7670–7681. https://doi.org/10.1523/JNEUROSCI.0629-11.2011.

25. Warwick, R.A., Kaushansky, N., Sarid, N., Golan, A., and Rivlin-Etzion, M. (2018). Inhomogeneous Encoding of the Visual Field in the Mouse Retina. Curr. Biol. *28*, 655–665.e653. https://doi.org/10.1016/j.cub.2018.01.016.

26. Joesch, M., and Meister, M. (2016). A neuronal circuit for colour vision based on rod-cone opponency. Nature *532*, 236–239. https://doi.org/10.1038/nature17158.

27. Zhang, Y., Kim, I.J., Sanes, J.R., and Meister, M. (2012). The most numerous ganglion cell type of the mouse retina is a selective feature detector. Proc. Natl. Acad. Sci. USA *109*, E2391–E2398. https://doi.org/10.1073/pnas.1211547109.

28. Kim, I.J., Zhang, Y., Yamagata, M., Meister, M., and Sanes, J.R. (2008). Molecular identification of a retinal cell type that responds to upward motion. Nature *452*, 478–482. https://doi.org/10.1038/nature06739.

29. El-Danaf, R.N., and Huberman, A.D. (2019). Sub-topographic maps for regionally enhanced analysis of visual space in the mouse retina. J. Comp. Neurol. *527*, 259–269. https://doi.org/10.1002/cne.24457.

30. Cumming, B.G., and Parker, A.J. (1999). Binocular neurons in V1 of awake monkeys are selective for absolute, not relative, disparity. J. Neurosci. *19*, 5602–5618.

31. Thomas, O.M., Cumming, B.G., and Parker, A.J. (2002). A specialization for relative disparity in V2. Nat. Neurosci. *5*, 472–478. https://doi.org/10.1038/nn837.

32. La Chioma, A., Bonhoeffer, T., and Hübener, M. (2020). Disparity Sensitivity and Binocular Integration in Mouse Visual Cortex Areas. J. Neurosci. *40*, 8883–8899. https://doi.org/10.1523/JNEUROSCI.1060-20.2020.

33. Mathis, A., Mamidanna, P., Cury, K.M., Abe, T., Murthy, V.N., Mathis, M.W., and Bethge, M. (2018). DeepLabCut: markerless pose estimation of user-defined body parts with deep learning. Nat. Neurosci. *21*, 1281–1289. https://doi.org/10.1038/s41593-018-0209-y.

34. Batschelet, E. (1981). Circular Statistics in Biology (Academic Press).

35. Dana, H., Chen, T.-W., Hu, A., Shields, B.C., Guo, C., Looger, L.L., et al. (2014). Thy1-GCaMP6 Transgenic Mice for Neuronal Population In Vivo. Plos One *9*, https://doi.org/10.1371/journal.pone.0108697.

36. Dombeck, D.A., Khabbaz, A.N., Collman, F., Adelman, T.L., and Tank, D.W. (2007). Imaging large-scale neural activity with cellular resolution in awake, mobile mice. Neuron *56*, 43–57. https://doi.org/10.1016/j.neuron.2007.08.003.

37. Scholl, B., Pattadkal, J.J., Dilly, G.A., Priebe, N.J., and Zemelman, B.V. (2015). Local Integration Accounts for Weak Selectivity of Mouse Neocortical Parvalbumin Interneurons. Neuron *87*, 424–436. https://doi.org/10.1016/j.neuron.2015.06.030.

38. Ohzawa, I., DeAngelis, G.C., and Freeman, R.D. (1990). Stereoscopic depth discrimination in the visual cortex: neurons ideally suited as disparity detectors. Science *249*, 1037–1041. https://doi.org/10.1126/science.2396096.

39. Cumming, B.G., and DeAngelis, G.C. (2001). The physiology of stereopsis. Annu. Rev. Neurosci. *24*, 203–238. https://doi.org/10.1146/annurev.neuro.24.1.203.

40. Hacker, M.J.R. (1979). R. A revised table of d' for M-alternative forced choice. Percept. Psychophys. *26*, 168–170.

Please cite this article in press as: Boone et al., Natural binocular depth discrimination behavior In mice explained by visual cortical activity, Current Biology (2021), https://doi.org/10.1016/j.cub.2021.02.031

CellPress

STAR★METHODS

KEY RESOURCES TABLE

REAGENT or RESOURCE	SOURCE	IDENTIFIER
Experimental Models: Organisms/Strains		
Mouse: C57Bl6J	The Jackson Laboratory	JAX: 00664
Mouse: C57BL/6J-Tg(Thy1-GCaMP6f) GP5.17Dkim/J	The Jackson Laboratory	JAX: 025393
Software and Algorithms		
Analysis code for the two-photon and pole descent tracking data	Figshare (https://figshare.com/projects/Natural_binocular_depth_discrimination_behavior_in_mice_explained_by_visual_cortical_activity/97846)	N/A
Discrimination analysis	[2]	N/A
Deposited Data		
PDCT behavioral performance	Mendeley Data (https://doi.org/10.17632/jgrktzy2hf.1).	N/A
Data for the two-photon and pole descent tracking data	Figshare (https://figshare.com/projects/Natural_binocular_depth_discrimination_behavior_in_mice_explained_by_visual_cortical_activity/97846)	N/A

RESOURCE AVAILABILITY

Lead Contact

Further information and requests for resources and reagents should be directed to and will be fulfilled by the lead contact, Aaron W. McGee (aaron.mcgee@louisville.edu).

Materials Availability

This study did not generate new reagents

Data and Code Availability

The data corresponding to the PDCT behavioral performance for Figure 1C are available at Mendeley Data (https://doi.org/10.17632/jgrktzy2hf.1). Data and analysis code for the two-photon and pole descent tracking data are available through Figshare (https://figshare.com/projects/Natural_binocular_depth_discrimination_behavior_in_mice_explained_by_visual_cortical_activity/97846).

EXPERIMENTAL MODEL AND SUBJECT DETAILS

Mice

Experiments and procedures were performed on both C57bl6 adult male and female mice (RRID: JAX: 00664). Mice were group housed and maintained on a 12 h light/dark cycle under standard housing conditions. All procedures and care were performed in accordance with the guidelines of the Institutional Animal Care and Use Committees at the University of Louisville and the University of Texas at Austin.

METHOD DETAILS

Monocular Deprivation (MD)

One eye was closed using a single mattress suture tied with 6-0 polypropylene monofilament (Prolene 8709H; Ethicon) under brief isoflurane anesthesia (2%) for durations described. The knot was sealed with cyanoacrylate glue. Prior to behavioral testing, the eye was examined while handling the mouse. Mice in which the suture did not hold overnight were re-sutured and examined again the following day.

Please cite this article in press as: Boone et al., Natural binocular depth discrimination behavior In mice explained by visual cortical activity, Current Biology (2021), https://doi.org/10.1016/j.cub.2021.02.031

Whisker clipping

The day prior to testing, mice were briefly anesthetized with isoflurane (5% induction, 1% maintenance) and the vibrissae clipped close the mystacial pad with iridectomy scissors. Mice recovered on a water jacket regulated by a thermostat in isolated cages and then were returned to group housing.

The Pole Descent Visual Cliff Task

The Pole Descent Visual Cliff (PDVC) task evaluates the preference of untrained mice to descend a pole to the closest of 4 platforms visible through a glass surface. The platform of the nearest quadrant is adjustable independently from the three remaining quadrants with lab-grade jacks (United Scientific Steel) positioned beneath platforms. The box housing the platforms is constructed with black High-Density Polyethylene (HDPE) Panels, connected using 2.5 × 2.5 cm T-slotted aluminum railing (80/20). Hinged doors are located on one side of the box to allow for adjustment of the platform(s) as needed. All interior surfaces and platforms were covered in a high-contrast pattern (vinyl decal paper with adhesive backing, patterned with 2.5 × 2.5 cm sized black and white checkerboard squares), aligning the pattern so that the edges of the squares were aligned. The top glass surface is 61 cm square with a centered circular 1.3 cm hole. A round plastic dowel (pole) 1 cm in diameter is attached to the base of the box and projects through the hole to a height of 51 cm about the glass. The pole is texturized with a rubberized coating (Flex Seal) to improve grip for the mice. A cone 7.6 cm high and 10 cm in diameter cut from a funnel rests on two cross beams of lightweight aluminum hexbar 0.3 cm in diameter (McMaster-Carr) and is positioned 2 cm above the glass surface. The testing box rests on a 16'' plastic turntable to permit repositioning of the target quadrant (McMaster-Carr). See Figure S2 for pictures and a diagram of the testing box.

Prior to testing, mice were individually handed for 2 days for 5 min each. During this period, mice were allowed to explore the open palm and gloved hands of the experimenter. On the day of testing, cages of mice were collected from the vivarium, placed on shelves outside the testing room, and acclimated for 1 h. Cohorts of male mice tested to completion, then cohorts of female mice were tested thereafter.

Cohorts of mice were tested in interleaved trials with the position of the nearest quadrant chosen at random. The quadrant was never in the same position for more than two consecutive trials. For each trial a mouse was collected from the cage with both hands, perched upon the open palm of the experiments, and then placed on the pole facing away from the experimenter such that the back legs grasped the pole approximately 2 cm from the top. Mice then climbed down the pole and exited to the platform. Outcomes were scored when the mice touched the glass with two front paws. Thereafter they were collected from the chamber. Mice were scored as follows for 15 trials: 1 = Mouse exited the pole to the quadrant with the closest platform; 0 = Mouse exited the pole to any other quadrant ; 'S' = Mouse slipped off the pole or cone; or 'T' = the mouse 'timed-out' because it did not exit the pole within three minutes. Following each trial, the pole, the cone, the aluminum rods, and the glass surface were cleaned with disinfectant wipes (Clorox® Multi-Surface Cleaning Wipes without Bleach) and the glass surface then cleaned with solution containing ammonia and 2-hexoxyethanol (Windex).

The average score for each mouse was calculated across 15 trials. If a mouse receives 3 consecutive scores of 'T', the mouse was not tested in subsequent trials. S and T scores were not factored into the fractional success. Only mice that completed 8 or more trials with a score of 0 or 1 for those trials were included the analysis. We excluded 8 percent of mice based on these criteria.

Videography of the Pole Descent Cliff Task

Video was captured of three additional mice performing multiple trials of the pole descent cliff task discriminating a 2.5 cm from 30.5 cm surface. Only correct trials were analyzed and to avoid dealing with occlusion from the cone, trials where the mouse had to choose one of the back two quadrants were excluded. This provided us with 14 videos and the tracking results from these videos were significantly consistent (Figures 1D and 1E). We also qualitatively observed this behavior across all of our experiments that were not captured with video. The head and body of the mice were tracked over time using DeepLabCut,[33] but we found the head to more reliably capture the position of the mouse, which was used for all subsequent steps. Markers were placed at the top of the pole and top of the cone, which were used to vertically orient the frames with respect to the pole and to convert pixels into cm. Considering a prior assumption of relative smooth changes in mouse position from frame to frame, we fit the DeepLabCut output to a polynomial of order 30. These smoothed horizontal and vertical coordinates of the head position of the mice were then converted into (1) an angular position with respect to the pole that captures horizontal and depth positions and (2) height from the cone. To simplify angle computations, the head was assumed 1 cm from the pole and progressively farther from the pole once reaching the cone based on the angle of the cone. Additionally, frames were hand scored on whether the mouse was in front of or behind the pole. This hand scoring correlated with the DeepLabCut confidence score, since the tracking was less confident when the mouse was partially occluded by the pole. With all of this information, we computed the angle of the mouse with respect to the pole, where zero degrees is directly to the right of the pole. This angle estimate was also smoothed to compensate for small head movements unrelated to body position on the pole. Height from the cone was then estimated from the vertical position and the angle. When the mouse is behind the pole, the height is reduced relative to the vertical position and when the mouse is in front of the pole, the height is increased relative to the vertical position. All angle results were rotated so that the near surface was always in the lower right quadrant (315 to 0 degrees). Angular deviation was computed versus height and compared to the deviation for a random distribution of angles of equal size.[34] Last, a histogram of positions was computed for on the pole (heights above 0) versus on the cone (heights below 0), and both histograms were compared to a random distribution of angles.

Please cite this article in press as: Boone et al., Natural binocular depth discrimination behavior In mice explained by visual cortical activity, Current Biology (2021), https://doi.org/10.1016/j.cub.2021.02.031

Calcium imaging of neuronal activity with two-photon microscopy

The imaging data compared to the behavioral data was previously published.[2] In summary, one male and two female C57BL/6J-Tg(Thy1-GCaMP6f)GP5.17Dkim/J mice that express GCamp6f under the Thy1 promoter were imaged head-fixed while awake and free to run on a floating trackball (RRID: JAX: 025393).[35,36] A titanium bar was affixed to the skull with dental acrylic and a 3-mm glass window was placed over the binocular region of V1 under isoflurane anesthesia (1%–3%). Excitation light from a mode-locked (920 nm) Chameleon Ultra Ti:Sapphire laser (Coherent Technologies) was focused with a 16x water objective (0.8 numerical aperture; Nikon) 150-250 μm below the surface and green light images (256 × 455 pixels) were collected with photomultiplier tubes at 30 Hz from a 400 –500 μm square region with a custom-built two-photon resonant mirror scanning microscope.[37]

Neuronal discrimination of depth

All neuronal response and discrimination analysis were performed consistent with our published methods.[2] To measure disparity-dependent responses, black and white dynamic random dot stereograms (70° x 100°, 6 Hz, 7.4° dot size, 400 dots) were shown to mice rear-projected onto an RP3D polarization-preserving screen (Severtson Screens) placed 22 cm in front of the mice with an Optoma HD27 projector and a circular polarization alternator (DepthQ/Lightspeed Design) with a refresh rate of 120 Hz. Passive circular polarization filters were placed in front of the mouse eyes to achieve stereoscopic presentation. Pixel intensities were summed within hand selected masks around cells based on size, shape, brightness and responsiveness. Responses to each 6 s stimulus presentation (interleaved with 6 s mean gray screen) were normalized by subtracting and dividing by the median response over the duration of an imaging session (ΔF/F). Significant visual responses ($p < 0.05$) were determined by comparing the paired difference between the mean response when the stimulus was on and the mean response in the preceding 2 s. Significant disparity tuning ($p < 0.05$) was determined with a Kruskal–Wallis test across presented disparities. Crossed (-) and uncrossed (+) disparities of 0°, 1.85°, 5.55°, and 9.20° were shown to mice and we fit Gabor functions to the responses to these disparities.[15,38,39] Eye position was continuously measured and there was no significant disparity-dependent change in binocular alignment. Gabor functions for cells were used to discriminate disparities estimated from the depths used in the pole descent cliff test. The preferred disparity for each cell was the maximum response. In our previous work, the task involved disparities that were always symmetric around zero disparity.[2] For the task in this study, the surfaces are not symmetric around zero disparity so cells were assigned as relative near or far based on the disparity in between the largest crossed and uncrossed disparity used in the task rather than being absolutely crossed or uncrossed. For the population of cells, all responses were normalized by the response to the preferred disparity and d' was computed by comparing the normalized responses to the two disparities for the surfaces the mice had to discriminate:[14]

$$d' = \frac{\mu\text{correct} - \mu\text{incorrect}}{\frac{1}{2}(\sigma^2\text{correct} + \sigma^2\text{incorrect})} \quad \text{(Equation 1)}$$

where *correct* are the responses for surfaces matched to the preference of the neuron and *incorrect* are the responses for surfaces mismatched to the preference of the neuron. For d' to increase, relative near cells should respond more to the surface with a crossed disparity or closer to crossed disparities and relative far cells should respond more to the surface with uncrossed disparity or closer to uncrossed disparities. The ratio of correct discriminations was estimated from d' measurements.[40] For variations in viewing distance or binocular eye alignment, disparity was recomputed for the five surfaces and tuning curves, and relative near and far disparity preference was reclassified.

QUANTIFICATION AND STATISTICAL ANALYSIS

For the Pole Descent Cliff Task, statistical comparisons were analyzed using Prism software (GraphPad). Values were reported as averages with standard error of means (SEM). Circles represent individual mice. Comparisons of the effects of distances and manipulations during testing were analyzed via a non-parametric Kruskal-Wallis test with Dunn's correction.

For the angular deviation and neuronal discrimination of depth, all statistical tests were nonparametric based on the median and error bars were based on bootstrap analysis of the median by resampled data 1000 times, allowing repeats, to produce surrogate datasets of the same size. The 160th and 840th samples were used for the SE of the median for all results.

Current Biology, Volume *31*

Supplemental Information

Natural binocular depth discrimination behavior

In mice explained by visual cortical activity

Howard C. Boone, Jason M. Samonds, Emily C. Crouse, Carrie Barr, Nicholas J. Priebe, and Aaron W. McGee

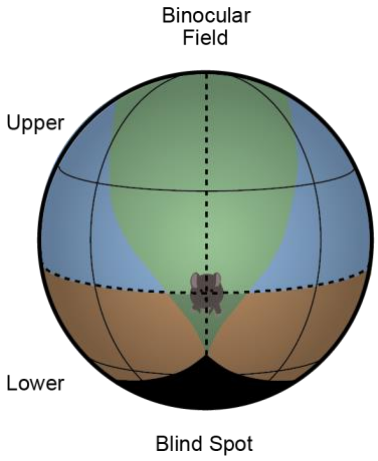

Figure S1. A three-dimensional depiction of the mouse visual field, Related to Figure 1.
The field is projected onto a global with the mouse within the center of that globe. Green represents where both eyes project (binocular overlap). Blue represents the upper half of the visual field and Brown represents the lower half of the visual field. There is greater binocular overlap in the upper field compared to the lower field.

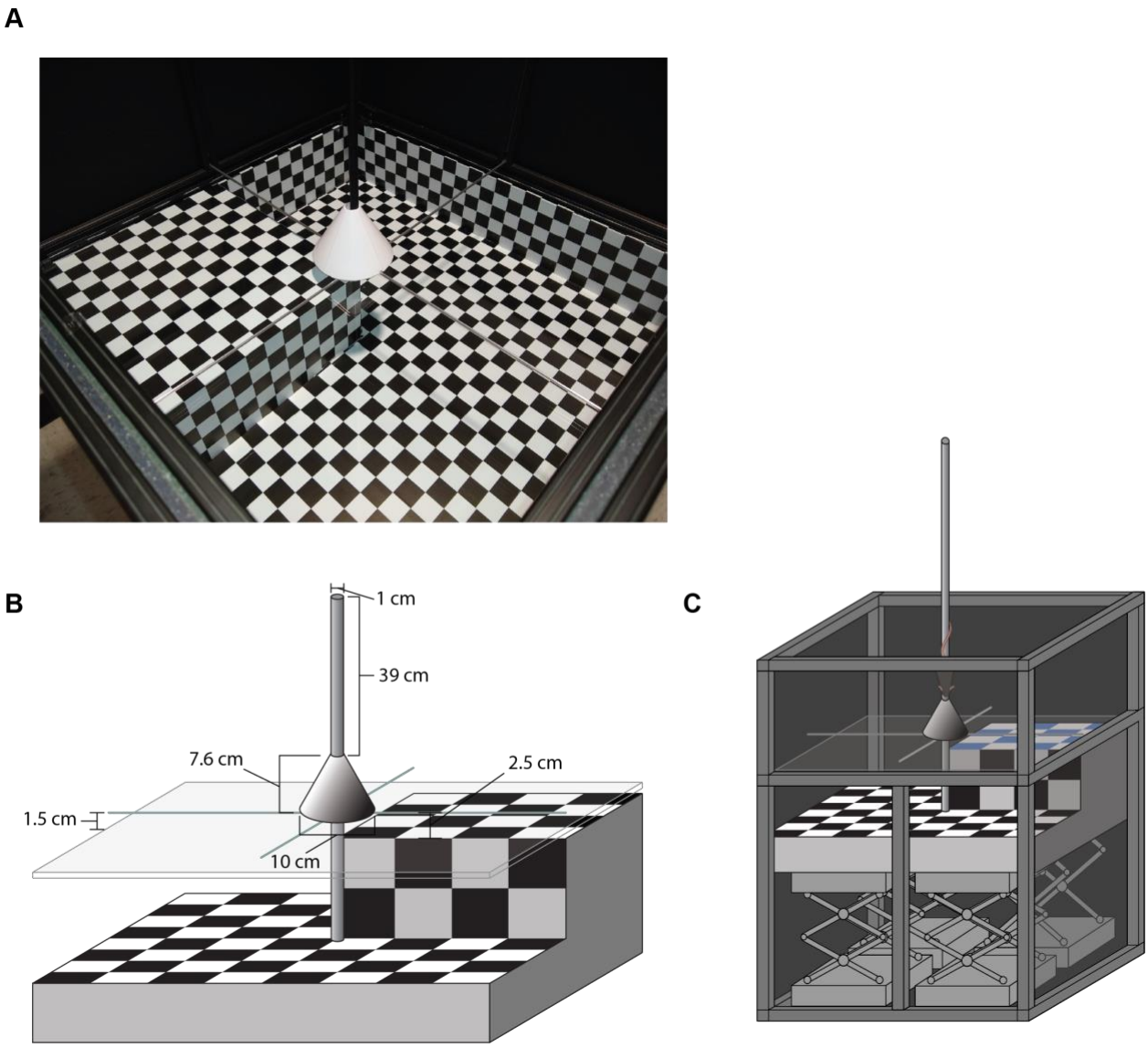

Figure S2. Image and Diagram of the Pole Descent Cliff Task (PDCT), Related to Figure 1
(**A**) Image of the PDCT. The quadrant and surface nearest the pole is at far right. The distance pairs presented are 2.5 cm (nearest quadrant) and 15.2 cm. All interior surfaces are covered with black and white 2.5cm checkerboard for all distance pairs. (**B**) Schematic of the PDCT with the dimensions for the central components (**C**) Diagram of the PDCT residing inside the testing box positioned on labjacks.

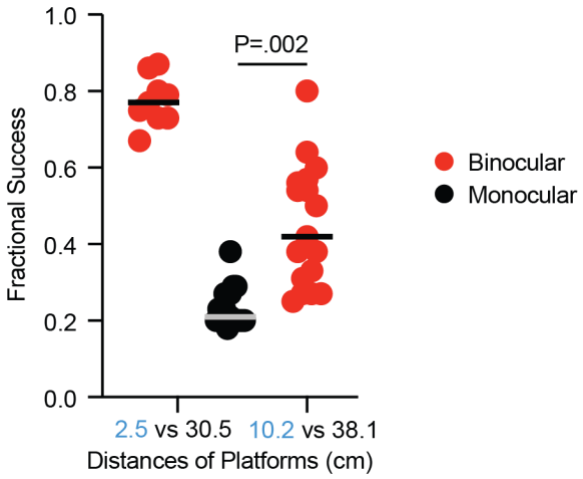

Figure S3. Discrimination analysis based on neuronal disparity tuning predicts reduced performance on the PDCT, Related to Figure 3. Mice (n=17) tested on the PDCT with both the nearest and more distant platforms displaced 7.6 cm farther away (10.2 cm and 38.2 cm, respectively) discriminate the nearest platform (P=.002), but at lower fractional success than 2.5 cm vs. 30.5.

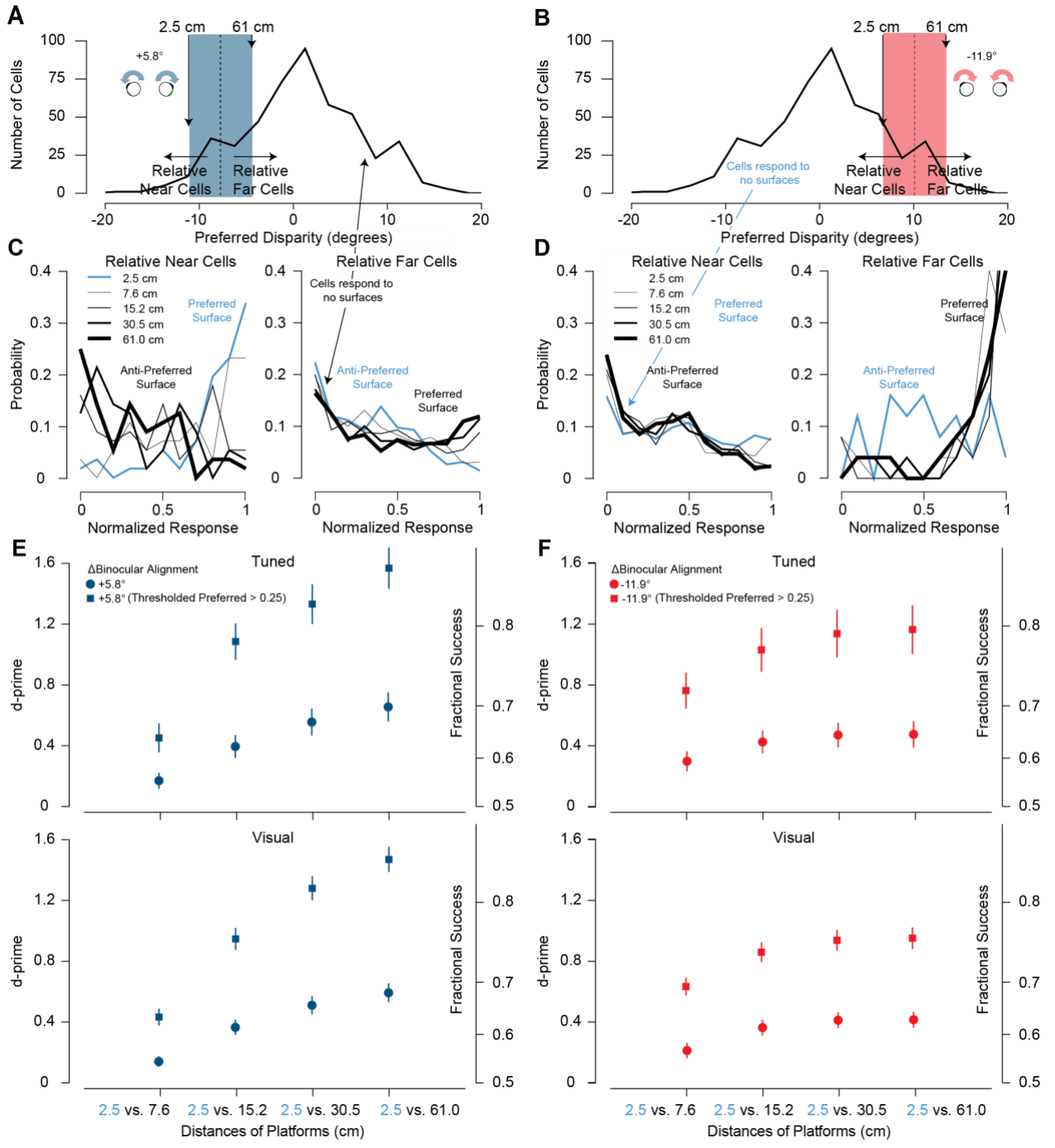

Figure S4. Neuronal Disparity Discrimination Improves by Applying a Response Threshold, Related to Figure 4.
(**A**) Blue shaded region of the disparity preference distribution highlights the range of disparities representing the PDCT surfaces when the eyes are 5.8 degrees more divergent. (**B**) Red shaded region of the disparity preference distribution highlights the range of disparities representing the PDCT surfaces when the eyes are 11.9 degrees more convergent. (**C**) Most relative far cells do not respond to any surface in the PDCT for the more divergent alignment. (**D**) Most relative near cells do not respond to any surface in the PDCT for the more convergent alignment. (**E**) and (**F**) Applying a threshold of a normalized response of 0.25 to surfaces matched to the preference (preferred surface) increases discrimination performance to levels that more closely match the behavior of the mice. This thresholding eliminates including neurons that respond to none of the surfaces from the d' calculation. All error bars are standard error.